Steel and Composite Structures, *Vol. 18, No. 4 (2015) 1001-1021*
DOI: http://dx.doi.org/10.12989/scs.2015.18.4.1001

Ultimate strength behavior of steel-concrete-steel sandwich beams with ultra-lightweight cement composite, Part 2: Finite element analysis

Jia-Bao Yan [a], J.Y. Richard Liew * and Min-Hong Zhang [b]

Department of Civil and Environmental Engineering, National University of Singapore, E1A-07-03, One Engineering Drive 2, Singapore 117576

(*Received December 13, 2013, Revised September 02, 2014, Accepted October 21, 2014*)

Abstract. Ultra-lightweight cement composite (ULCC) with a compressive strength of 60 MPa and density of 1,450 kg/m^3 has been developed and used in the steel-concrete-steel (SCS) sandwich structures. This paper investigates the structural performances of SCS sandwich composite beams with ULCC as filled material. Overlapped headed shear studs were used to provide shear and tensile bond between the face plate and the lightweight core. Three-dimensional nonlinear finite element (FE) model was developed for the ultimate strength analysis of such SCS sandwich composite beams. The accuracy of the FE analysis was established by comparing the predicted results with the quasi-static tests on the SCS sandwich beams. The FE model was also applied to the nonlinear analysis on curved SCS sandwich beam and shells and the SCS sandwich beams with J-hook connectors and different concrete core including ULCC, lightweight concrete (LWC) and normal weight concrete (NWC). Validations were also carried out to check the accuracy of the FE analysis on the SCS sandwich beams with J-hook connectors and curved SCS sandwich structure. Finally, recommended FE analysis procedures were given.

Keywords: cement composite; finite element analysis; J hook connector; overlapped connector; sandwich structure

1. Introduction

Steel-concrete-steel (SCS) sandwich composite structure with ultra-lightweight cement composite has been developed for potential applications in building and offshore constructions (Yan 2012, Yan *et al*. 2014a, b, c). The newly developed ultra-lightweight cement composite (ULCC) with compressive strength of 60 MPa and lightweight density 1,450 kg/m^3 was used as the core material to reduce the overall self-weight of the SCS sandwich structure (Sohel *et al*. 2010, Wang *et al*. 2013, Yan *et al*. 2014a, b, c). Overlapped headed shear studs were chosen to bond the steel face plates and the cement composite core to form an integrated unit. The overlapping headed studs, as shown in Fig. 1, not only provide shear resistance against longitudinal slip at the

∗Corresponding author, Professor, E-mail: ceeljy@nus.edu.sg
[a] Research Fellow, E-mail: ceeyanj@gmail.com
[b] Professor, E-mail: mhzhang@nus.edu.sg

http://www.techno-press.org/?journal=scs&subpage=8 ISSN: 1229-9367 (Print), 1598-6233 (Online)

interacting interface, but also provide transverse shear resistance to the sandwich beam section. This paper investigates the structural performance of this sandwich composite beam using nonlinear finite element (FE) analysis method in which the structural behaviour of the overlapping headed shear studs are modelled carefully so that their influence on the ultimate strength behavior of SCS sandwich beams can be captured with good accuracy.

The shear resistance of the headed shear studs has been studied extensively by numerical methods by Nguyen and Kim (2009), Mirza and Uy (2010), Chang *et al*. (2011), Guezouli and Lachal (2012), Guezouli *et al*. (2013), and Pavlovic *et al*. (2013). In their FE models, the headed shear studs were modelled using three dimensional continuum elements. The full geometry simulation of the headed studs led to more elements at the headed stud zone and more complex contacting interaction between the headed stud and concrete, which finally resulted in time consuming and convergence problem of the FE analysis. These FE models are suitable for analyzing push-out or pull-out test specimens of which only several studs (usually less than six) needed to be modelled explicitly. For the cases of the SCS sandwich beams or plates, there are much more connectors and thus the modelling of all the connectors would increase the computational effort tremendously. Detailed modeling of the headed studs as well as its neighborly interacting concrete requires very fine element meshes. The numerical solution can be terminated abruptly due to convergence problem associated with cracking and crushing of concrete at the contact surfaces. Full geometry FE simulation of the shear connectors in the steel-concrete composite beams has also been carried out by using 3D continuum elements (Lam and El-Lobody 2001, Qureshi *et al*. 2011). Explicit type of solver was used for the FE analysis to solve the aforementioned convergence problems caused by the fine mesh, steel-concrete contact interaction, and material nonlinear behaviors of concrete. This method was proven to be effective in simulating the steel-concrete interaction, but it requires very small time step in the explicit solver to achieve convergence and thus incurs significant computational time. A simplified FE model was developed by using an anisotropic element that considered the transverse shear contribution of the connectors (Kumar 2000, Shanmugam *et al*. 2002). Though this model could capture the ultimate strength of the structure, it cannot fully capture the structural interaction between the connector and concrete core, and thus cannot predict shear failure of the connectors in the structure. Foundoukos and Chapman (2008) developed two dimensional models for the FE analysis of the Bi-steel structures and it has the limitation on the simulation of three dimensional behaviors of the shear connectors in concrete. More recently, truss element, spring element, or cohesive materials

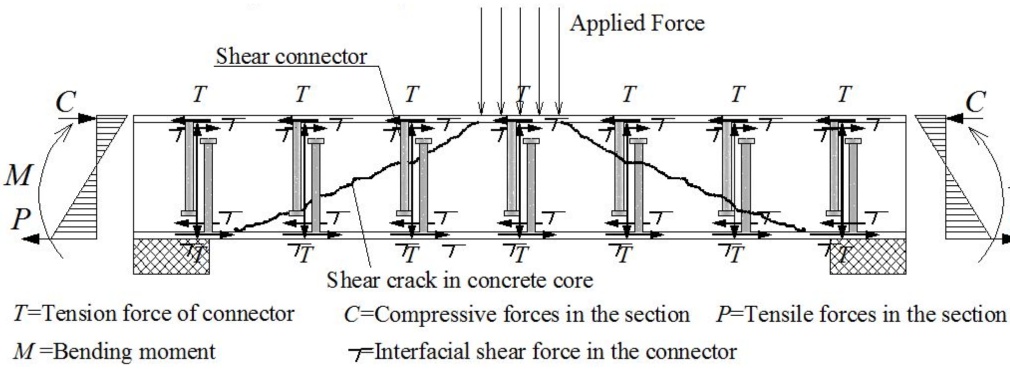

Fig. 1 Illustration of functions of the overlapped headed shear studs in the structure

were used to simulate the connectors' behavior at the steel-concrete interface (Song *et al*. 2010, Luo *et al*. 2012, Zhao and Li 2008). Although these models can capture the longitudinal shear-slip behavior of the headed shear studs in the beam structure, they fail to capture the tension elongation behavior of the stud connectors when the steel plate is separated from the concrete core due to tension force.

The experimental studies on the ultimate strength behavior of the SCS sandwich beams have been reported by the authors in Part 1 of the paper (Yan *et al*. 2014b). This second-part paper focuses only numerical modelling and nonlinear analysis on this type of structure. In the present investigation, three dimensional nonlinear FE model was developed in which nonlinear spring element linking two cylindrical studs at the center was used to represent a pair of overlapping headed shear studs and to account for shear and tension transfer at the steel and concrete interface. The validity of FE model was established by comparing the numerical results with tests conducted on nine SCS sandwich beams. This FE model was further extended to analyze the ultimate strength behavior of SCS sandwich beams with J-hook connectors and curved SCS sandwich beam and shell structures. The accuracy of the FE analyzes was confirmed by the validations against the test results of the SCS sandwich beams with J-hook and curved SCS sandwich beams and shell structure.

2. Finite element model

General finite element (FE) program ABAQUS was used to model the SCS sandwich composite beams with overlapped headed shear studs (ABAQUS 2009). Considering the geometric and loading symmetry of the SCS sandwich composite beam, only one-fourth of the full model was built. The main components for the SCS sandwich composite beams in the FE model are steel face plates, concrete core, connectors, load cell, and support.

2.1 Behaviours of headed shear stud

In the SCS sandwich composite structures with overlapped headed shear studs, the headed shear studs were used to transfer longitudinal shear forces at the steel-concrete interface and bridge the shear cracks in the core material, as shown in Fig. 1. They also provide resistance against outward buckling of the steel plate subjected to compression due to flexural action. The headed shear studs usually work in pairs with an overlapped length in the SCS sandwich composite beams.

2.2 Modeling of overlapped headed shear stud

Since the strength and force deformation behaviour of connectors have significant influence on the global behaviour of SCS sandwich composite structure, their longitudinal shear-slip behaviors and axial tension-elongation behaviors should be properly simulated in the FE model. Full geometry simulation of the headed shear studs needs fine element meshes at the head zone of the studs and the adjacent concrete. This would increase the number of the elements and the chance of increasing the elements that may be highly distorted. In addition, the full geometry simulation of the headed shear studs also leads to more contact pairs of the interacting surfaces. All these increased number of elements and interacting contact surfaces result in convergence problems.

Therefore, a simplified model that can capture the behavior of a pair of overlapped headed stud connectors is necessary, and the interfacial shear-slip behaviors and tension-elongation behaviors of the connector should be captured in the FE model.

A new method was developed to model a pair of overlapped headed shear stud connectors in the SCS sandwich structure by using two rods linked at the center by a nonlinear spring element as shown in Fig. 2. The rods were modelled by solid elements with the same diameter, material property as the headed studs in the SCS sandwich beam. The spring element has a physical length of 5 mm with predefined tension-elongation behavior of overlapped headed shear studs obtained from tensile tests. It was also assigned a much larger linear compression stiffness to make sure the rods taken the compression and avoid the spring element failing in compression.

Three tensile tests were carried out as shown in Fig. 3(a). The tensile test comprises a pair of overlapped headed shear studs that were embedded in the ultra-lightweight cement composite (ULCC). The studs used in the tensile tests were with the same geometry and material properties as used in the SCS sandwich beams tests. Two steel bars were clamped and tensioned until the connectors were pulled out from the cement core or the cement core failed. The relative elongations between the top steel face plate and the bottom steel face plates were recorded by the linear varying displacement transducers (LVDTs). These obtained tension-elongation behaviors for the three specimens are shown in Fig. 3(b).

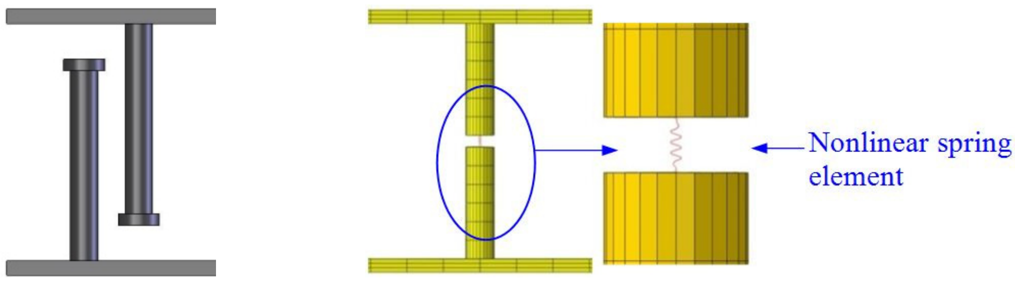

(a) (b)

Fig. 2 Simulation of the overlapped headed shear stud by the spring element

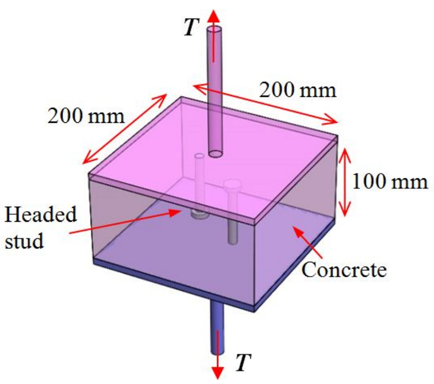

(a) Tension test on overlapped headed studs

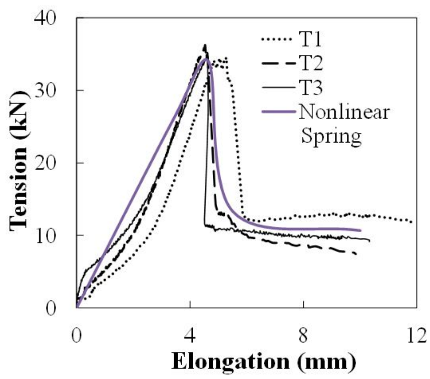

(b) Tension-elongation curve

Fig. 3 Tension-elongation behavior of overlapped headed studs

These tension-elongation behaviors were then assigned to the spring element that links the top and bottom connectors in the structure. The defined tension-elongation behavior for the nonlinear spring element was compared with the tensile tests results in Fig. 3(b). It can be observed that the spring element can capture the tension-elongation behaviors of the overlapped headed shear stud connectors used in the sandwich beam.

2.3 Finite element model

2.3.1 Element type

Three-dimensional eight node continuum element with reduced integration point and hourglass control (C3D8R) was employed to model the shear connectors, concrete core and steel face plates (as shown in Fig. 4) (ABAQUS 2009). Nonlinear spring model was used to connect the two overlapped connectors. Considering the symmetry of the SCS sandwich composite beam, only one quarter of the beam was modeled. Different mesh sizes were used to make a balance between the FE analysis accuracy and computing processing time. The different mesh sizes for the concrete core, steel plate and connectors are shown in Fig. 5. The FE model of SCS beam is shown in Fig. 6.

2.3.2 Contact, boundary conditions and applied load

Different contact pairs were defined for different interacting components of SCS sandwich

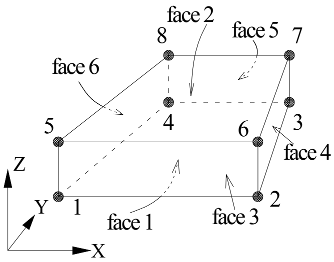

Fig. 4 C3D8R element in FE model

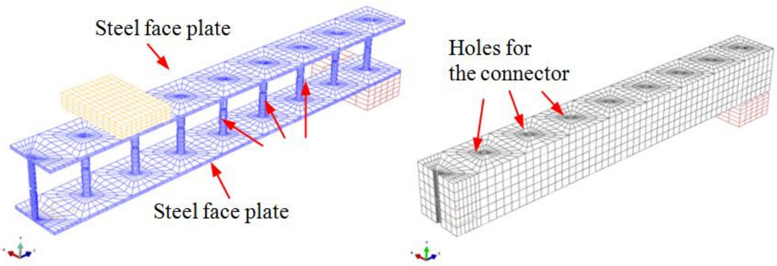

Fig. 5 Different mesh size for different components and locations in FE model

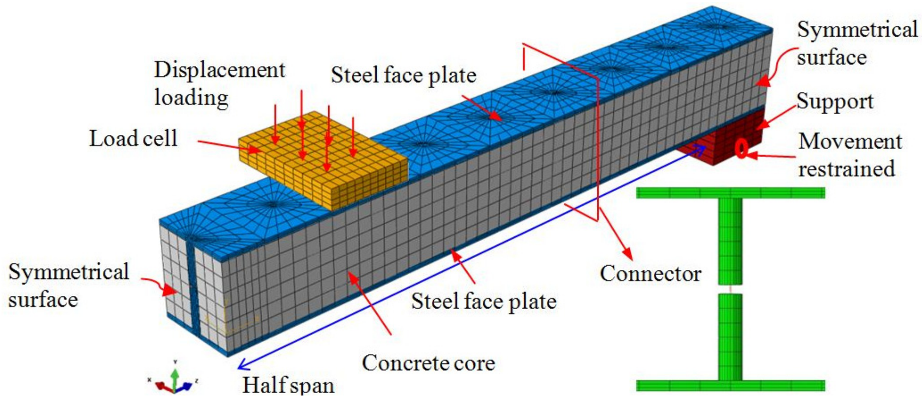

Fig. 6 FE model of SCS sandwich beam with headed shear studs

composite beam. General contact interaction with "hard contact" formulation in normal direction and "penalty" friction formulation in tangential direction was used between the steel face plates and concrete core, load cell and top steel face plates, and supports and bottom steel face plates. Friction coefficient 0.5 was used in this contact formulation as recommend by Qureshi *et al.* (2011). General contact interaction with "hard contact" formulation in normal and frictionless in tangential direction was used to simulate the interaction between the concrete core and the connectors.

As shown in Fig. 6, symmetric boundary conditions were applied on the surface along the longitudinal centerline and surface at the mid-span. The end support was restrained to move in any direction but can rotate along its centerline that simulates the simply pin support. Displacement controlled loading was applied to the load cell which transfers the load to the beam.

2.3.3 Material models

The concrete damage plasticity model in ABAQUS was chosen for the core materials in the SCS sandwich composite beams. This model is defined by two failure mechanisms of axial compressive crushing and tensile cracking of the concrete. The uniaxial compressive behavior of the concrete was obtained from the compression tests on concrete cylinder specimens. The compressive stress-strain curve for the ULCC obtained from the compression tests was used in the FE model as shown in Fig. 7(a). The ultimate compressive strength and elastic Young's modulus are 60 MPa and 16.5 GPa, respectively. Other parameters including flow potential eccentricity of 0.6, dilation angle of 36°, and ratio of the biaxial/uniaxial compressive strength ratio of 1.16 were set for this plastic damage model. For the tension capacity of the core material, linear elastic tensile behavior is assumed before the crack develops. The cracked concrete can be simulated by the nonlinear stress-strain behavior or fracture energy cracking model. The ultimate tensile strength of the ULCC was obtained through the splitting tensile tests on the cylinders. For the fracture energy parameter, it can be calculated by the following equation in CEB-FIP (1993)

$$G_f = G_{f0}\left(\frac{f_{ck}}{10}\right)^{0.7} \tag{1}$$

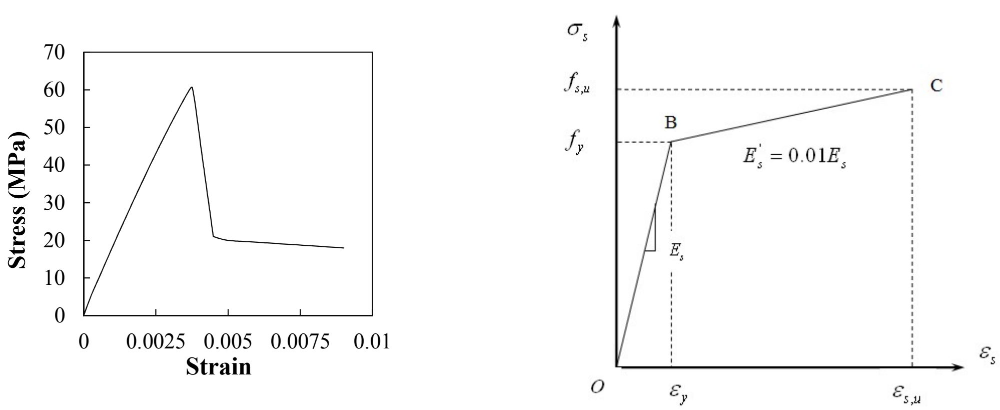

(a) Stress-strain curve of ULCC (b) Stress-strain curve of steel material

Fig. 7 Stress-strain curves of the ULCC and steel material in the FE

Table 1 Material properties of steel face plates and headed studs

Item	B1	B2	B3	B4	B5	B6	B7	B8	B9
f_y (MPa)	275	305	310	305	305	305	305	305	310
f_u (MPa)	419	450	450	450	455	450	450	450	450
σ_y (MPa)	495	495	495	495	495	495	495	495	495
σ_u (MPa)	527	527	527	527	527	527	527	527	527

* f_y = yield strength of steel face plate; f_u = ultimate strength of steel face plate;
σ_y = yield strength of headed stud; σ_u = ultimate strength of headed stud

Table 2 Details of the SCS sandwich composite beams

Beam	t (mm)	S (mm)	L (mm)	Core material	f_{ck} (MPa)	E_c (GPa)	u (kg/m^3)	Failure mode	P_u (kN)	Failure mode	P_E (kN)	P_E / P_u
B1	4.0	100	500	ULCC	67.4	17.3	1441	CSF, BSY	212.3	CF, CSF	221.8	1.04
B2	6.0	100	500	ULCC	65.2	17.3	1450	CSF	236.0	CF, CSF	241.0	1.02
B3	12.0	100	500	ULCC	69.3	17.3	1450	CSF, BSY	378.0	CSF	403.2	1.07
B4	6.0	100	500	LWC	24.1	12.7	1324	CSF	133.6	CSF	135.1	1.01
B5	6.0	100	500	HPC	180.0	60.0	2672	CSF	451.3	CSF	462.2	1.02
B6	6.0	150	500	ULCC	67.2	17.3	1521	CF, CSF	233.1	CF, CSF	233.7	1.00
B7	6.0	200	500	ULCC	64.6	17.3	1440	CF, CSF	165.4	CF, CSY	162.6	0.98
B8	6.0	100	1100	ULCC	67.2	17.3	1521	CSF, BSY	174.3	CSF, BSY	171.7	0.99
B9	5.7	100	1600	ULCC	64.6	17.3	1440	FF, BSY	127.8	FF, BSY	121.9	0.95
Mean												1.01
Cov												0.03

*t = thickness of the steel plate; S = spacing of the connectors in the beam; L = span of the beam;
E_c = secant modulus of elasticity;u = density of the concrete core;
σ_u = ultimate strength of the connectors; $_y$ = yield strength of the steel plates;
*BSY = Bottom steel plate yield; CSF = concrete core shear failure; CF = connector shear failure;
FF = flexural failure; P_u = ultimate strength of the test;
P_E = ultimate strength by FEA (finite element analysis); Cov = coefficient of variation

where G_f = the fracture energy, Nmm/mm^2; G_{f0} varies as the coarse aggregate of the concrete changes, G_{f0} = 0.025 Nmm/mm^2 for the d = 8 mm coarse aggregate, G_{f0} = 0.030 Nmm/mm^2 for the d = 16 mm, G_{f0} = 0.058 Nmm/mm^2 for the d = 32 mm; d is diameter of the coarse aggregate in the concrete, mm; f_{ck} = compressive strength of the concrete cylinder, MPa.

Since ULCC is a new material and there is no test data available on the fracture energy, a smallest value G_{f0} = 0.025 Nmm/mm^2 is used for ULCC considering there is no coarse aggregate in it, and G_f = 0.088 Nmm/mm^2 is used in the tensile behavior of the plastic material model for the ULCC.

Elastic-plastic isotropic material model was used for both the steel face plates and headed shear studs. This bi-linear material model (as shown in Fig. 7(b)) consists of two parts that define the elastic and plastic behavior of the steel material, respectively. In the elastic part, the elastic Young's modulus E and Poisson's ratio μ were defined for the steel plate and connectors. For the plastic part as shown in Fig. 7(b), the ultimate strength as well as the corresponding strain was defined in this model. Tension tests on steel coupons of the steel plates and connectors were carried out to obtain the Young's modulus E, yield strength, and ultimate strength. In the FE analysis, E = 205 GPa and μ = 0.3 were used for both steel plate and connectors. The yield strength and ultimate strength for the steel face plates and the connectors were listed in Table 1.

3. Validation of the finite element model

The FE analyses were validated by the quasi-static tests on nine SCS sandwich beams carried out by the authors (Yan *et al*. 2014b).

3.1 Description of the beam tests

The details of the beams are listed in Table 2. All these nine SCS sandwich beams were designed with the overlapped headed shear studs. The width of the sandwich beam and height of the concrete core were 250 and 100 mm, respectively. Beams B1-B7 were designed with span of 600 mm whilst the spans for B8 and B9 were 1100 and 1600 mm, respectively.

The test setups for beams B1-9 are shown in Fig. 8.

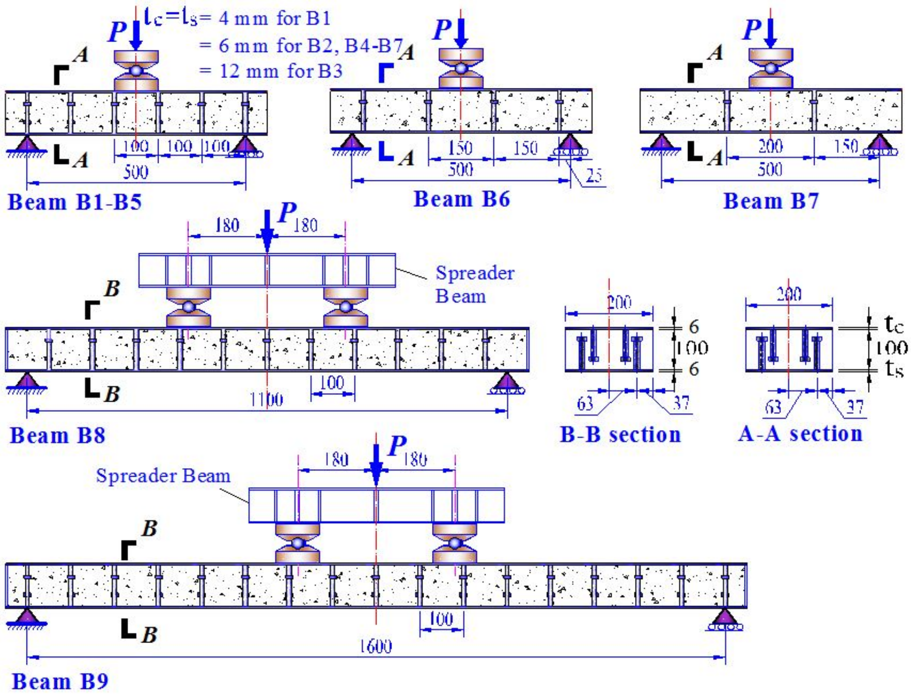

Fig. 8 Test setup and details of the sandwich beam

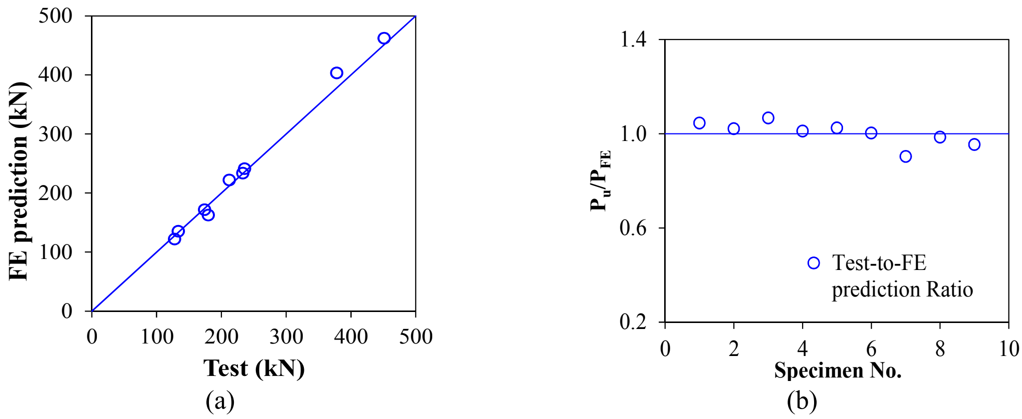

Fig. 9 Comparisons of experimental results and FEA

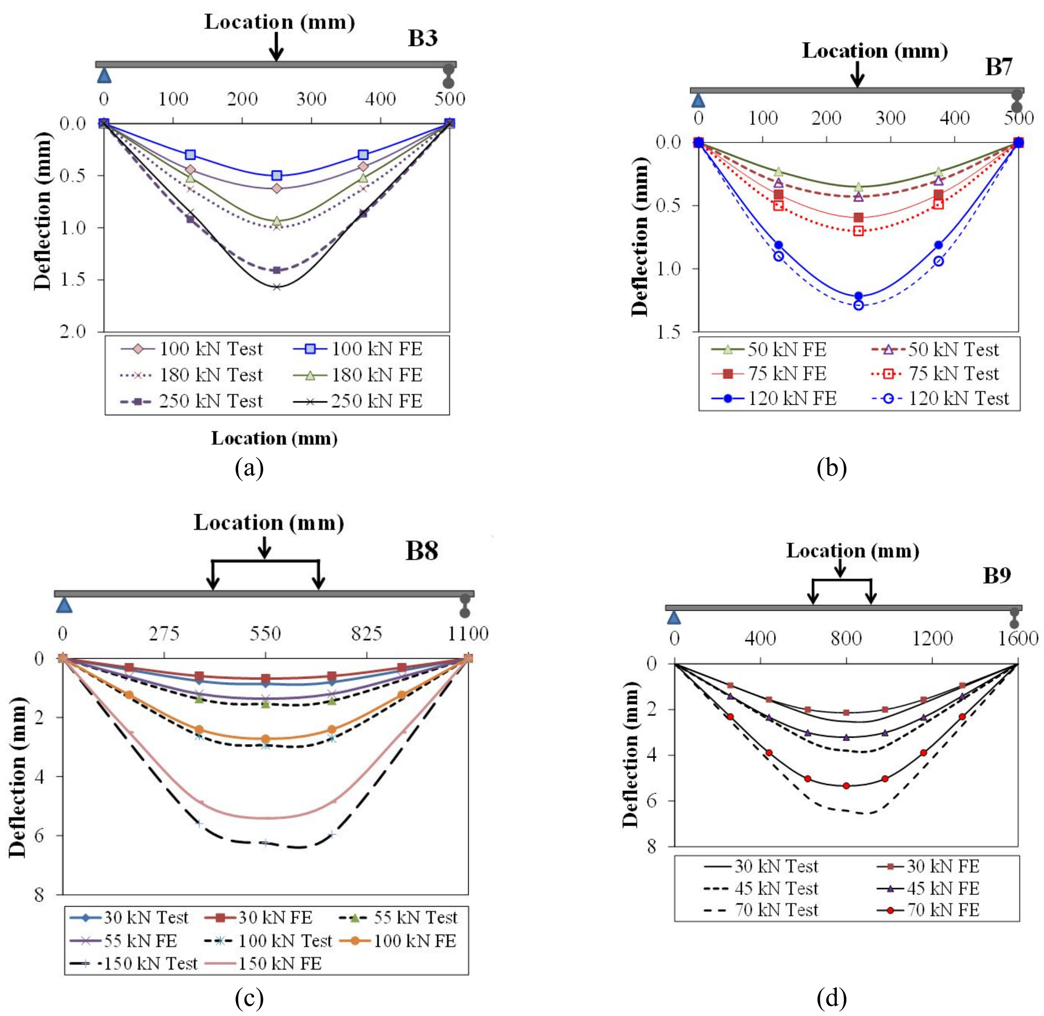

Fig. 10 Comparisons of experimental results and FEA

3.2 Ultimate strength and failure mode

The ultimate strength and failure modes of the finite element analysis (FEA) are compared with the test results in Table 2 and Fig. 9. From these table and figures, it can be seen that reasonably good agreements of the FEA are exhibited compared with test results. The average test-to-FE prediction ratio of ultimate strength is 1.02 with a coefficient of variation (COV) of 0.03. Moreover, the FEA predicted most of the exact failure modes that were observed during the test.

3.3 Deformed shape

The deformed shapes of the SCS sandwich beams B3, B7, B8, and B9 at different load levels until service load limit obtained by the FEA are compared with the experimental ones in Fig. 10.

It can be observed that the FEA can predict the deformed shape of the SCS sandwich beam

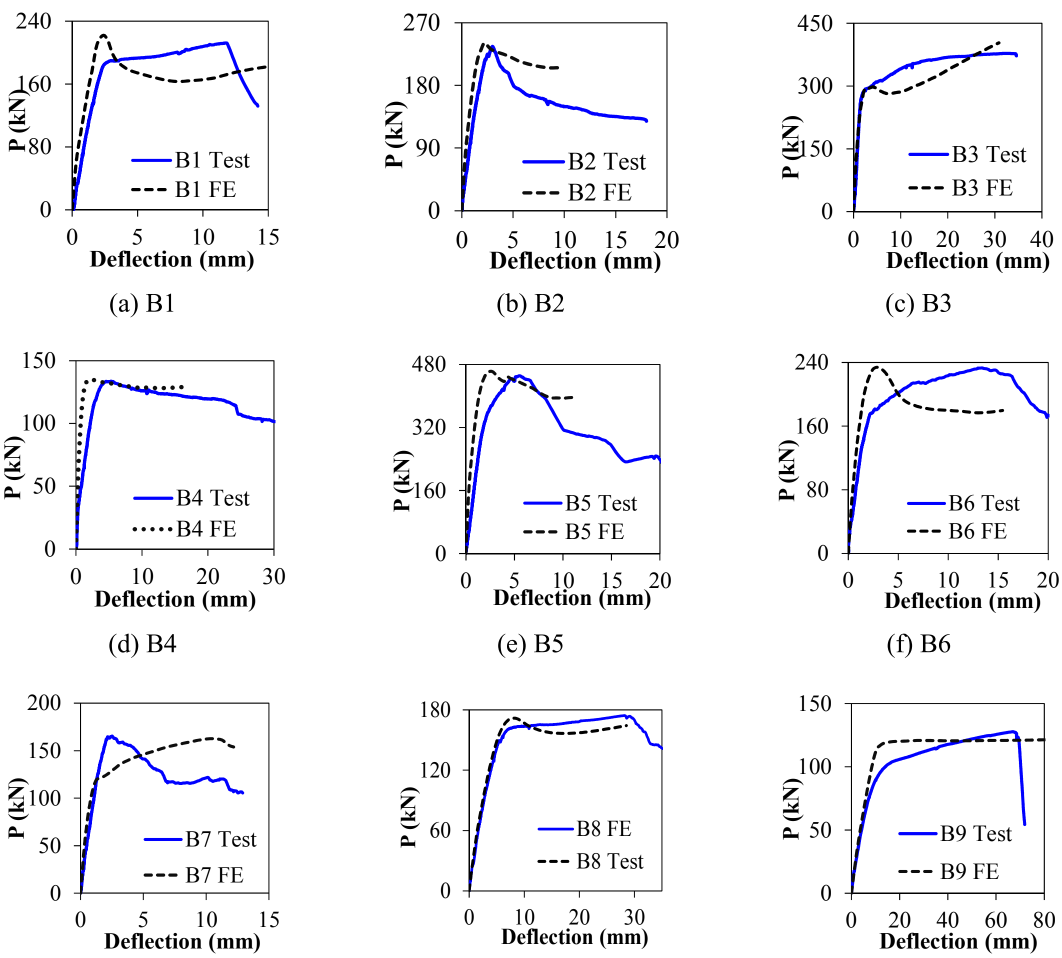

(a) B1 (b) B2 (c) B3

(d) B4 (e) B5 (f) B6

(g) B7 (h) B8 (i) B9

Fig. 11 Comparisons of the load-central deflection curves between the tests and FEA

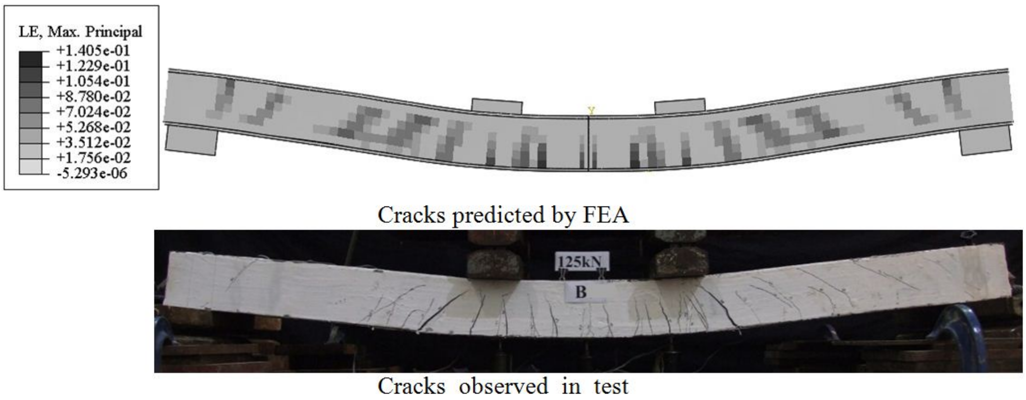

(a) Beam B9

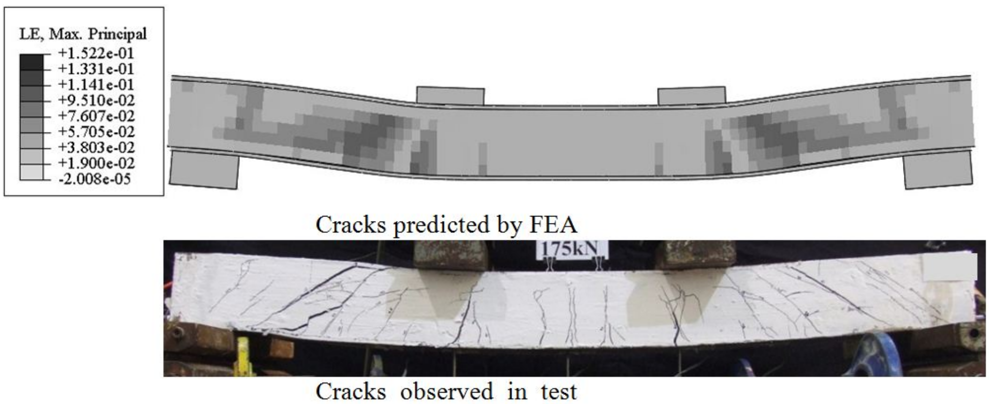

(b) Beam B8

Fig. 12 Comparisons of the cracks in the core between the FEA and test

under service loads (250, 110, 116, and 85 kN for B3, B7, B8, and B9, respectively) with error less than 20 percent. Under the service load, the predicted deflections are smaller than the experimental results. This may be caused by the soft support during testing. The sandwich specimens were supported on two steel girders under the test frame which resulted in additional deflection.

3.4 Load-central deflection behavior

The mid-span deflection versus applied load of specimens B1 to B9 obtained by the FEA were compared with the experimental curves in Figs. 11(a)-(i).

From these figures, it can be observed that the load-central deflection curves of the FEA exhibit reasonably good agreements with the experimental curves though there are some mismatch on the nonlinear part and post peak behavior of the curves. The differences in the post peak load-deflection curves may be attributed to the stiffeners at the support, limited data on the fracture energy of the ULCC core material, and simplified material model of the overlapped headed shear stud connectors.

3.5 Cracks in the concrete core

The cracking in the concrete core can be predicted by monitoring the principle strain contour of the concrete core. Once the limit of the cracking strain is exceeded, cracks are assumed to be developed. The cracked concrete element are highlighted and compared with the crack patterns observed from the tests in Fig. 12. It can be observed that the crack patterns predicted by the FE model compared well with those observed from the tests.

3.6 Load-end slip behaviors between the bottom steel face plate and concrete core

The load-end slip behaviors between the concrete core and bottom steel face plate given by the FEA were compared with the corresponding experimental load-slip curves in Fig. 13. The proposed FE model offers reasonable predictions of the load-slip behavior between the steel face plate and the concrete core when they were subjected to static loading with acceptable differences. It was also observed from the test that sometimes the slip was too small to be measured especially at the initial elastic stage of the SCS sandwich beam. This might be one reason that caused the differences of the load-slip curves between the predictions and the test results. Another reason may be the influences of the stiffeners that welded at the two ends of the beam, which was initially used to enhance shear capacity of the beam at support location to avoid shear failure of the SCS sandwich beam at the supports.

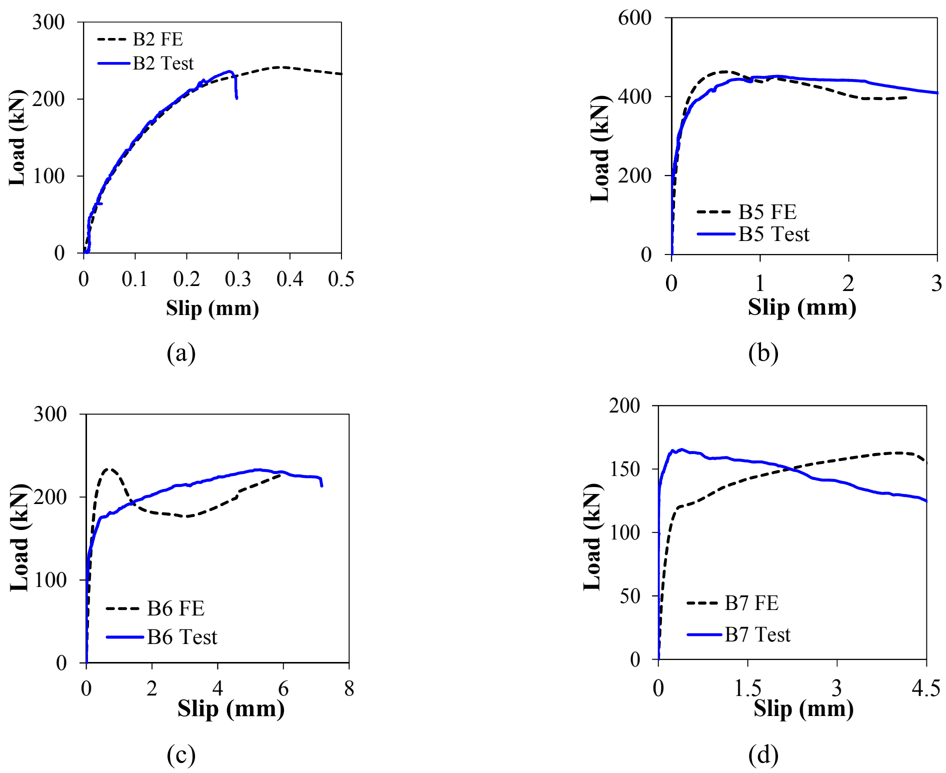

Fig. 13 Load-slip behavior between the steel face plate and concrete

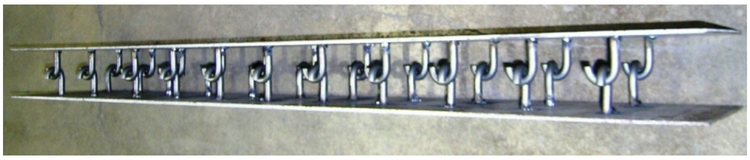

(a) SCS sandwich beam with J-hook connectors

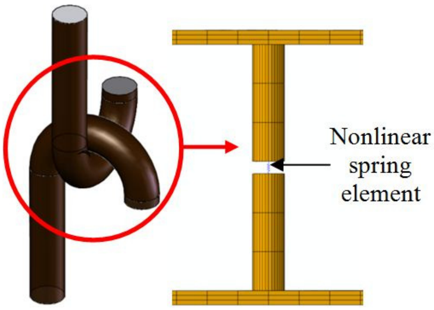

(b) Simulation of the J-hook connectors in the FE model

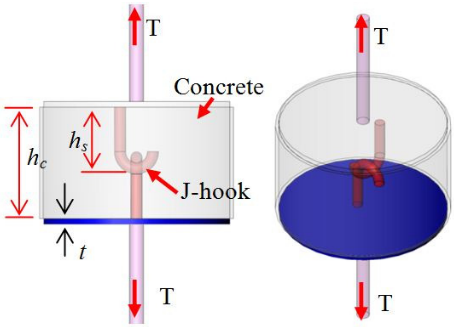

(c) Tensile test on the J-hook connectors

Fig. 14 Simulations of the J-hook connectors in the FE model

4. Discussions and applications

4.1 Discussions

From the verification works shown in Section 3, the proposed FE model is shown to be capable of predicting the structural behaviors of the SCS sandwich beams with overlapped headed shear stud connectors in terms of the failure mode, ultimate strength, load-deflection behavior, deformed shapes, interfacial slip between the steel face plate and concrete core, and crack patterns in the concrete core.

The proposed FE model can be also applied to the structures with other types of interlocked or overlapped shear connectors that work in pairs. The key elements are the simulations on the structural behaviors of the basic component, i.e., a pair of connectors. The simulated structural behaviors include longitudinal shear-slip behavior and axial tension-elongation behaviors. For the longitudinal shear-slip behavior of a pair of overlapped connectors, the embedding depth and diameter of the connectors were simulated in the FE model. For the axial tension-elongation behavior, tensile tests need to be carried out to obtain the necessary information to build the FE model.

The FE model developed in this paper can be used for the analysis of the SCS sandwich composite beams with J-hook connectors in which the J-hook connectors have similar function as the overlapped headed studs in the SCS sandwich beams. Moreover, this developed FE model can be used in the analysis on the ultimate strength behavior of the other forms of SCS sandwich structure with overlapped headed shear studs, e.g. curved SCS sandwich beam and shell structure. All these applications of the FE model will be presented in the following sections.

4.2 Applications of the FE model on SCS sandwich beams with J-hook connectors

Table 3 Details of the SCS sandwich beam with J-hook connectors

Beam	t (mm)	h_c mm	B mm	D mm	S mm	Core	V_f %	w kg/m^3	f_{ck} MPa	f_y MPa	σ_u MPa
SCS 80	4.0	80	240	10	80	NWC	-	2350	48.3	275	405
SLSC80	4.0	80	240	10	80	LWC	-	1445	28.5	275	405
SCS 100	4.0	80	200	10	100	NWC	-	2350	48.3	275	405
SLCS100	4.0	80	200	10	100	LWC	-	1445	28.5	275	405
SLFCS100	4.0	80	200	10	100	LWC	1S$^+$	1450	28.1	275	405
SCS150	4.0	80	300	10	150	NWC	-	2350	48.3	275	405
SLCS150	4.0	80	300	10	150	LWC	-	1445	28.5	275	405
SLCS200	3.9	80	200	16	200	LWC	-	1445	27.4	275	405
SLF200-1	3.9	80	200	16	200	LWC	1P$^+$	1450	28.7	275	405
SLF200-2	3.9	80	300	16	200	LWC	2P$^+$	1450	28.2	275	405
SLF300-1	3.9	80	200	16	300	LWC	1P$^+$	1450	28	275	405
J1	4.0	100	200	12	100	ULCC	0.5 P$^+$	1441	60.0	275	460
J2-1	6.0	100	200	12	100	ULCC	0.5 P$^+$	1450	60.0	310	460
J2-2	6.0	100	200	12	100	LWC	-	1324	24.	310	460
J2-3	6.0	100	200	12	100	HPC	-	2672	160	310	460
J3	12.0	100	200	12	100	ULCC	0.5 P$^+$	1481	60	310	460
J4	6.0	100	200	12	150	ULCC	0.5 P$^+$	1521	60	310	460
J5	6.0	100	200	12	200	ULCC	0.5 P$^+$	1440	60	310	460
J6	6.0	100	200	12	100	ULCC	0.5 P$^+$	1481	60	310	460
J7	6.0	100	200	12	100	ULCC	0.5 P$^+$	1482	60	310	460

*t = thickness of the steel plate under compression; B = width of the beam cross section;
D = diameter of the J-hook; S = spacing of the connector; w = density of the concrete;
V_f = volume fraction of the fibre in the concrete; f_y = yield strength of the steel plate;
f_{ck} = compressive strength of the concrete cylinder; σ_u = ultimate strength of J-hook connector;
S$^+$ denotes steel fiber; P$^+$ denotes polyvinyl alcohol fiber

As discussed in Section 4.1, the J-hook connectors used in the SCS sandwich beams (as shown in Fig. 14(a)) may be used to replace the overlapped headed shear studs (Liew and Sohel 2009). SCS sandwich composite structure exhibits many advantages including no restriction on the depth of the panel, increasing the overall structural integrity, and exhibiting good structural performances under different loading cases especially under impact and fatigue loadings (Liew *et al*. 2009, Dai and Liew 2010). This type of structure has similarities to the SCS sandwich beam with overlapped headed studs. A pair of interlocked J-hook connectors plays the same function to the overlapped headed studs. Therefore, the proposed FE model can be used for the nonlinear analysis of the structural performance of the SCS sandwich beams with J-hook connectors.

4.2.1 Simulation of the J-hook connectors in the SCS sandwich beam

Following the same model as the overlapped headed stud connector, the J-hook connectors was simulated by two cylindrical studs linked by the nonlinear spring element as shown in Fig. 14(b).

Table 4 Details of the tensile test specimens on J-hook connector

Specimen	t (mm)	h_s (mm)	h_c (mm)	d (mm)	Fiber by volume	σ_y (MPa)	σ_u (MPa)	f_{ck} (MPa)	Material Type
TN1	6	58.8	100	11.8	-	310	480	47.7	NWC
TL1	6	56.3	95	11.8	-	310	465	30.0	LWC
TU1	6	56.3	95	11.8		310	465	65.2	
TU2	6	71.3	125	11.8		310	465	65.2	
TU3	4	57.3	95	11.8		310	465	65.2	
TU4	8	55.3	95	11.8	0.50%	310	465	65.2	ULCC
TU5	12	53.3	95	11.8		310	465	65.2	
TU6	6	60.5	95	16.0		280	405	65.2	

*NWC denotes normal weight concrete; NWFC denotes normal weight concrete with fibers; LWC denotes light weight concrete; LWFC denotes light weight concrete with fibers; ULCC denotes ultra-lightweight cement composite; t, h_s, and h_c are as shown in Fig. 14(c)

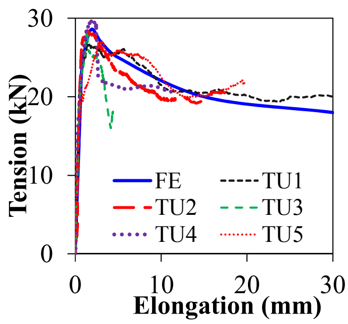

(a)

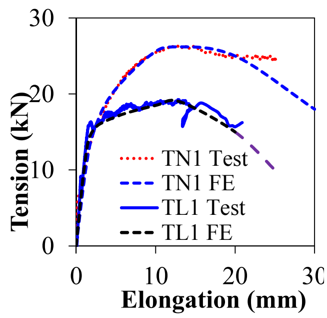

(b)

Fig. 15 Comparisons of tension-elongation behaviors of J-hook connectors between the tests and FE simulations

Twenty SCS sandwich beam specimens were tested and they were used to validate the FE model. The details of the beams were listed in Table 3.

In order to simulate the pair of J-hook connectors, tensile tests on the J-hook connectors were carried out. The test setup for the tensile tests is as shown in Fig. 14(c). Several specimens with the typical diameter of the J-hook connectors and concretes are shown in Table 4. The tension-elongation curves that were obtained from the tensile tests for a pair of interlocked J-hook connectors with different diameters and concretes types were compared with FE simulated tension-elongation behaviors in Fig. 15. From this figure, it can be seen that the axial tensile behavior of the J-hook connectors used in the FE model matches well with the experimental results that means the spring element used in the FE model could capture this behavior.

4.2.2 FE model for the SCS sandwich beam with J-hook connectors

The FE model for the SCS sandwich beams with J-hook connectors is similar to the SCS sandwich beam as shown in Figs. 5-6. The FE model includes the steel face plates, concrete core, support, connectors with linking spring element, and load cell.

4.2.3 Validation of the finite element analysis

The validations of the FEA include the comparisons of the ultimate load carrying capacities and load-central deflection curves with the test results.

Maximum resistance

The predicted ultimate load carrying capacities of the twenty SCS sandwich beam specimens

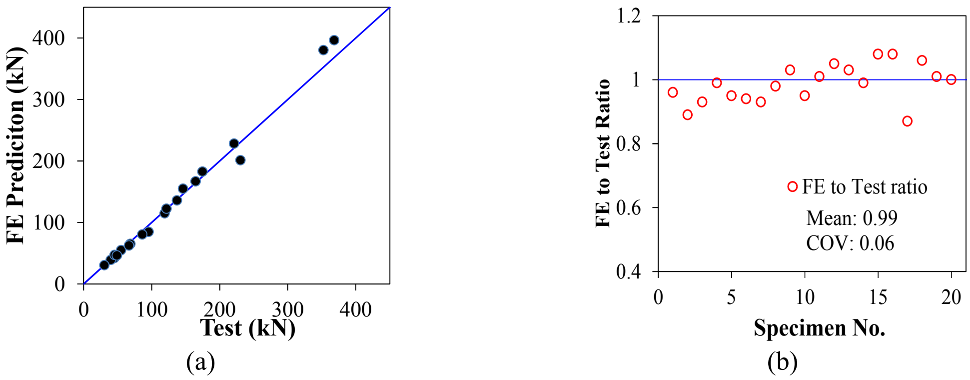

Fig. 16 Validations of the ultimate load carrying capacities

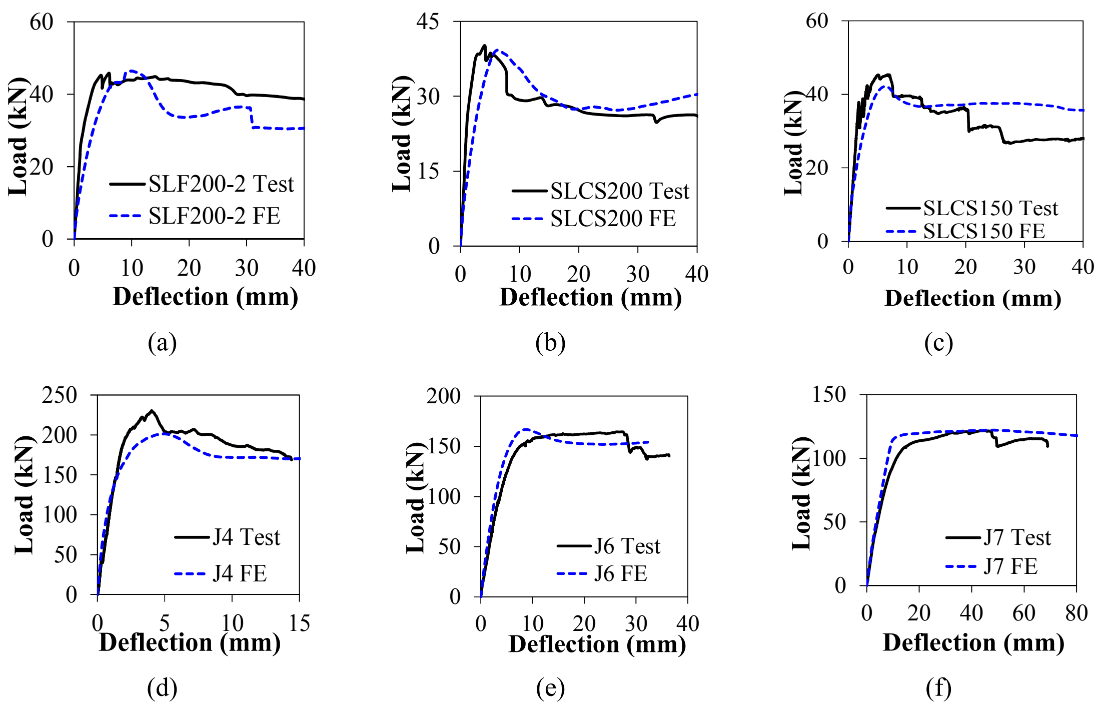

Fig. 17 Validations of the load-central deflection curves

were compared with the test results in Fig. 16. It is observed that the average prediction to test strength ratio is 0.99 with a coefficient of variation (COV) of 0.06. Thus it can be concluded that the FE model is capable of predicting the ultimate load carrying capacity of the SCS sandwich beam with J-hook connectors.

Load deflection behaviour

The load-central deflection curves that were obtained from the beam tests were compared with those by the FEA in Figs. 17 (a)-(f). From these figures, it can be observed that the predicted load-central deflection curves by the FEA agree well with the experimental curves in terms of elastic stiffness, and load deflection up to the maximum load, although some mismatch in post peak behaviour is observed for specimens SLF200-2 and SLCS150.

4.3 Application of the FE model in curved SCS sandwich beam and shell structures

This developed FE model can also be used in the analysis of the ultimate strength behavior of the curved SCS sandwich beams and shells. In these FE analyses, explicit type of solver was used.

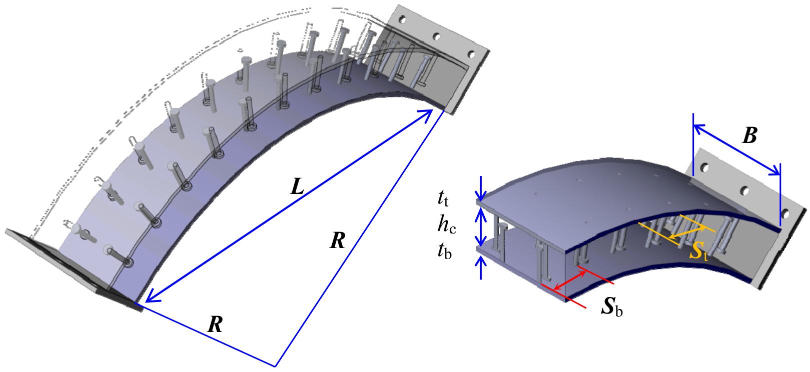

(a) Details of the curved SCS sandwich beam

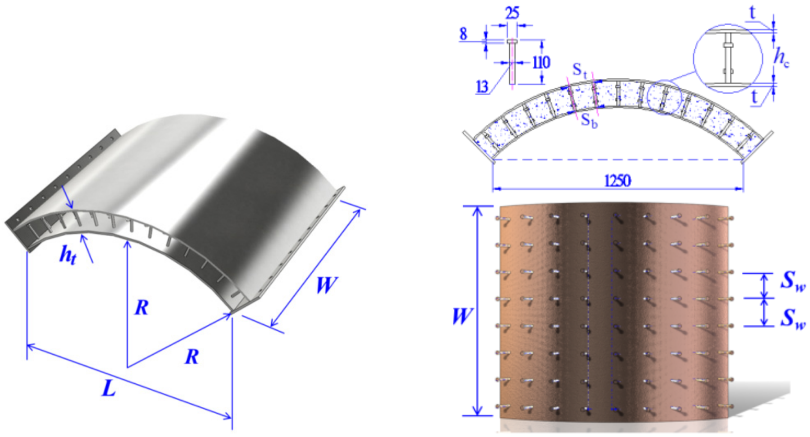

(b) Details of SCS sandwich shell

Fig. 18 Details of the curved SCS sandwich beam and shell structure

Table 5 Details of the curved SCS sandwich beams and shell

Specimen	R (mm)	L (mm)	$t_t = t_c$ (mm)	B/W (mm)	S_b (mm)	S_t (mm)	S_w (mm)	d (mm)	f_y (MPa)	σ_u (MPa)
CB1	888	1250	4	300	128	145	-	13	301	572
CB2	888	1250	12	300	128	145	-	13	390	572
CS1	888	1250	12	1250	200	228	208	13	340	503

*f_y deonotes yield strength of the steel face plate; σ_u deonotes ultimate strength of the connector

The two curved SCS sandwich beams were tested under the strip loading (100x300mm^2) along the width of the beam at the middle span. The SCS sandwich shell was tested under square patch loading (125 × 125 mm^2) at the geometry center of the top steel face shell.

4.3.1 Description of the tests on curved SCS sandwich beam and shell

The details of the two curved SCS sandwich beams (i.e., CB1 and CB2) and one curved SCS sandwich shell (CS1) are as shown in Fig. 18 and listed in Table 5. ULCC were used in these three specimens with the compressive strength and elastic Young's modulus of 60 MPa and 16.5 GPa, respectively.

4.3.2 Finite element model for the curved SCS sandwich beam and shell

Fig. 19 depicts the FE models used for the curved SCS sandwich beam and shell structure. Similarly to the FE models for the flat SCS sandwich beams, the overlapped headed shear stud were simplified by cylindrical connectors linked by the nonlinear spring element.

Considering the symmetry, only one quarter of the beam or shell was built in the FE model.

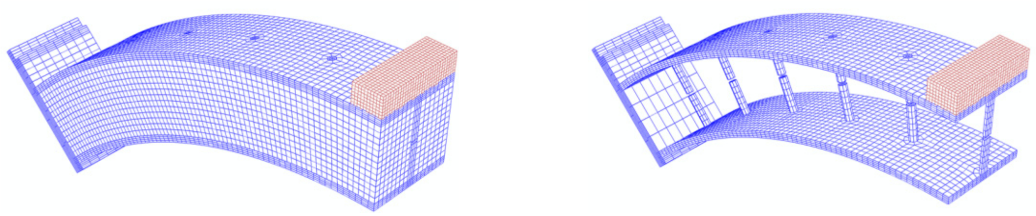

(a) FE model for the curved SCS sandwich beam

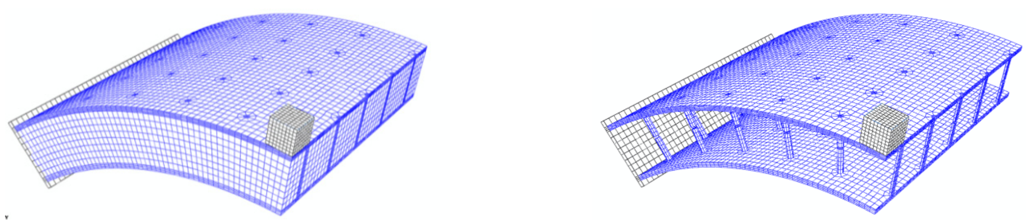

(b) FE model for the SCS sandwich shell

Fig. 19 Finite element model for the curved SCS sandwich beam and shell

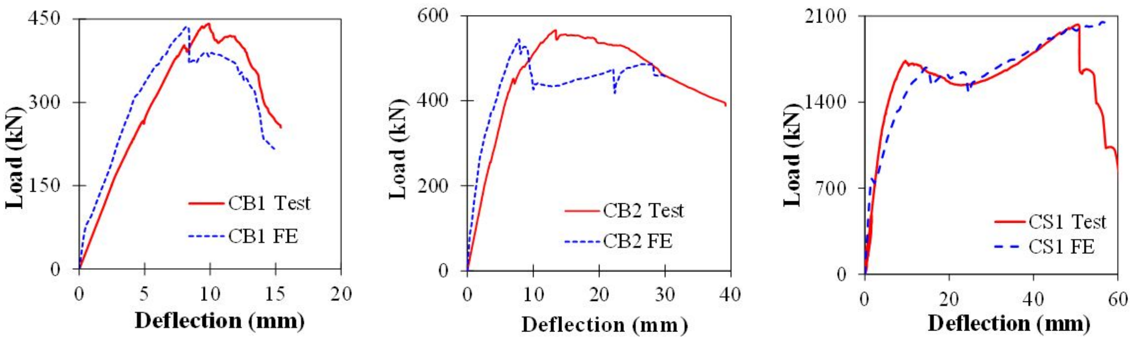

(a) (b) (c)

Fig. 20 Validations of the FE analysis on curved SCS sandwich beam and shell

4.3.3 Validations of the finite element analysis

The load-central deflection curves obtained from the FE analyzes are compared with the test ones in Fig. 20. It can be seen that the FE curves resembles well with the test results though there are some mismatches in the post peak behavior. Regarding the ultimate resistances, the FE analyzes give 1%, 4%, and 2% errors in predictions for CB1, CB2, and CS1 respectively compared with the test results.

5. Recommended finite element analysis procedures

To provide proper simulations on the behaviors of the shear connectors is very important in the FE analysis of the SCS sandwich structures. The developed FE model should capture the basic longitudinal shear-slip behavior and axial tension-elongation behaviors of the connectors. The longitudinal shear behaviors can be captured through modelling the cylindrical stud with the same diameter and height. The axial tension-elongation behaviors of the spring connector must be carefully calibrated against the data obtained from tensile tests. Therefore, tensile tests on the connectors used in the sandwich structure are necessary to ensure that the proposed FE model will work. The recommended FE analysis procedures were given as the following:

(1) Carrying out tensile tests on a pair of overlapped headed shear studs or interlocked J-hook connectors to get the tension-elongation behaviors. The tension-elongation behaviors will be used for the definition of the nonlinear spring element connecting the two cylindrical stud connectors.
(2) Modeling the steel face plates with the same geometry and materials as used in the beams.
(3) Modeling the cylinder shear stud pairs with the same diameter, embedding depth, and materials as the headed studs or J-hook connectors. The shear studs were tied to or merged with the steel face plates.
(4) Using the nonlinear spring element to link a pair of shear studs attached to the top and bottom steel face plates. The experimental tension-elongation behaviors of the connectors in step (1) are used for the defining tension-elongation behaviors of the spring elements.
(5) Building the concrete cores and defining the interactions among different interacting parts.
(6) Run the analysis and ensure convergence of solutions.

6. Conclusions

This paper develops a nonlinear-three dimensional-FE model for the analysis on the ultimate strength behavior of the SCS sandwich beams with interacted connectors that work in pairs, i.e., headed shear studs with overlapped length and interlocked J-hook connectors. In this FE model, two cylindrical studs linked by the nonlinear spring element were used to simulate a pair of overlapped headed studs or interlocked J-hook connectors. This simplified FE model proved to be capable of providing simulations on the longitudinal shear-slip behavior and axial tension-elongation behaviors of a basic unit in the SCS sandwich structure. More importantly, this developed FE model significantly reduced the number of the elements, simplified the interaction between the connectors and concrete, and avoided the elements being distorted. All these advantages increased the computational efficiency and improved the convergence of the FE analysis.

The ultimate load carrying capacity, load-central deflection curves, deformed shapes at different loading levels, relative slip between the steel plate and the concrete core, and cracks in the concrete core were predicted by the FE analysis and these predictions agreed well with experimental results of nine SCS sandwich beams with overlapped headed studs. Other experimental results comprising twenty beam tests on sandwich beams with J-hook connectors, two curved SCS sandwich beams and one SCS sandwich shell with overlapped headed studs were used to validate the FE model. All these validations proved that the developed FE model can precisely predict the ultimate strength behavior of the SCS sandwich structure with interacted connectors. Some minor errors of the FEA in the post peak behavior might be caused by the assumed shear-slip behavior and tension-elongation behaviors for the interacted connectors, limited information on the tensile fracture energy of the ULCC, and ignoring the confining effect of the concrete to the tensile and shear resistances of the connectors.

This developed FE model can be used for the analysis of ultimate strength behavior of SCS sandwich structures with other forms of interacted shear connectors. Based on the extensive validations, standard FE analysis procedures were recommended but tensile tests are necessary to establish the tension-elongation behavior of new types of connectors for the FE model of the SCS sandwich structures. The proposed FEA may be used to generate data needed to design SCS sandwich composite structures.

Acknowledgments

The research described herein was funded by the Maritime and Port Authority of Singapore, and supported by the American Bureau of Shipping (ABS) and National University of Singapore under research project titled “Curved steel-concrete-steel sandwich composite for Arctic region” (Project No. R-302-501-002-490).

References

ABAQUS (2009), User manual Version 6.9; DS SIMULIA Corp., Providence, RI, USA.

CEB-FIP (1993), CEB-FIP model code 1990; Comité Euro-International Du Béton, Redwood Books, Trowbridge, Wiltshire, UK.

Chang, X., Chen, H., Liu, B. and Zhao, F. (2011), “Modeling of anchor bolt pullout in concrete based on a

heterogeneous assumption", *Nucl. Eng. Des.*, **241**(5), 1345-1351.
Dai, X.X. and Liew, J.Y.R. (2010), "Fatigue performance of lightweight steel–concrete–steel sandwich systems", *J. Constr. Steel Res.*, **66**(2), 256-276.
Foundoukos, N. and Chapman, J.C. (2008), "Finite element analysis of steel–concrete–steel sandwich beams", *J. Constr. Steel Res.*,**64**(9), 947-961.
Guezouli, S. and Lachal, A. (2012), "Numerical analysis of frictional contact effects in push-out tests", *Eng. Struct.*, **40**, 39-50.
Guezouli, S., Lachal, A. and Nguyen, Q.H. (2013), "Numerical investigation of internal force transfer mechanism in push-out tests", *Eng. Struct.*, **52**, 140-152.
Kumar, G. (2000), "Double skin composite construction", Master Thesis; National University of Singapore, Singapore.
Lam, D. and El-Lobody, E. (2001), "Finite element modelling of headed stud shear connectors in steel-concrete composite beam", *Struct. Eng. Mech. Computat.*, **1**, 401-408.
Liew, J.Y.R. and Sohel, K.M.A. (2009), "Lightweight steel–concrete–steel sandwich system with J-hook connectors", *Eng. Struct.*, **31**(5), 1166-1178.
Liew, J.Y.R., Sohel, K.M.A. and Koh, C.G. (2009), "Impact tests on steel–concrete–steel sandwich beams with lightweight concrete core", *Eng. Struct.*, **31**(9), 2045-2059.
Luo, Y.J., Li, A. and Kang, Z. (2012), "Parametric study of bonded steel–concrete composite beams by using finite element analysis", *Eng. Struct.*, **34**, 40-51.
Mirza, O. and Uy, B. (2010), "Effects of the combination of axial and shear loading on the behaviour of headed stud steel anchors", *Eng. Struct.*, **32**(1), 93-105.
Nguyen, H.T. and Kim, S.E. (2009), "Finite element modeling of push-out tests for large stud shear connectors", *J. Constr. Steel Res.*, **65**(10-11), 1909-1920.
Pavlović, M., Marković, Z., Veljković, M. and Buđevac, D. (2013), "Bolted shear connectors vs. headed studs behaviour in push-out tests", *J. Constr. Steel Res.*, **88**, 134-149.
Qureshi, J., Lam, D. and Ye, J.Q. (2011), "Effect of shear connector spacing and layout on the shear connector capacity in composite beams", *J. Constr. Steel Res.*, **67**(4), 706-719.
Shanmugam, N.E., Kumar, G. and Thevendran, V. (2002), "Finite element modeling of double skin composite slabs", *Finite Elem. Anal. Des.*, **38**(7), 579-599.
Sohel, K.M.A. (2008), "Impact performance of steel-concrete-steel sandwich structures", Ph.D. Thesis; National University of Singapore, Singapore.
Sohel, K.M.A. and Liew, J.Y.R. (2011), "Steel-concrete-steel sandwich slabs with lightweight core-Static performance", *Eng. Struct.*, **33**(3), 981-992.
Song, T.Y., Han, L.H. and Uy, B. (2010), "Performance of CFST column to steel beam joints subjected to simulated fire including the cooling phase", *J. Constr. Steel Res.*,**66**(4), 591-604.
Wang, J.Y., Chia, K.S., Liew, J.Y.R. and Zhang, M.H. (2013), "Flexural performance of fiber-reinforced ultra lightweight cement composites with low fiber content", *Cement Concrete Compos.*, **43**, 39-47.
Yan, J.B. (2012), "Ultimate strength behaviors of steel-concrete-steel sandwich beams and shells", Ph.D. Thesis; National University of Singapore, Singapore.
Yan, J.B., Liew, J.Y.R., Sohel, K.M.A. and Zhang, M.H. (2014a), "Push-out tests on J-hook connectors in steel–concrete–steel sandwich structure", *Mater. Struct.*, **47**(10), 1693-1714.
Yan, J.B., Liew, J.Y.R., Zhang, M.H. and Wang, J.Y. (2014b), "Ultimate strength behavior of steel-concrete-steel sandwich beams with ultra-lightweight cement composite, Part 1: Experimental and analytical study", *Steel Compos. Struct.*, *Int. J.*, **17**(6), 907-927.
Yan, J.B., Liew, J.Y.R. and Zhang, M.H. (2014c), "Tensile resistance of J-hook connectors in steel-concrete-steel sandwich composite structure", *J. Constr. Steel Res.*, **100**, 146-162.
Zhao, G.Z. and Li, A. (2008), "Numerical study of a bonded steel and concrete composite beam", *Comput. Struct.*, **86**(19-20), 1830-1838.

CC